Cellular/Molecular

Electrical Coupling between Locomotor-Related Excitatory Interneurons in the Mammalian Spinal Cord

Christopher A. Hinckley and Lea Ziskind-Conhaim
Department of Physiology and Center for Neuroscience, University of Wisconsin Medical School, Madison, Wisconsin 53706

Locomotor rhythm generation is a fundamental characteristic of neural networks in the spinal cord. Identifying the synaptic interactions between neurons in the locomotor circuitry is key to our understanding of the mechanisms that underlie the production of rhythmic motor outputs. Using transgenic mice in which the homeobox gene *HB9* drives the reporter green fluorescent protein (GFP), we have demonstrated that a genetically distinct cluster of Hb9/GFP-expressing interneurons (Hb9 INs) can generate locomotor-like rhythms in the newborn mouse spinal cord (Hinckley et al., 2005b). Processes of Hb9 INs are in close apposition to adjacent Hb9 INs, raising the possibility that the interneurons are synaptically interconnected. To test this hypothesis, whole-cell paired recordings were performed from visually identified Hb9 INs. High-incidence bidirectional electrical coupling was evident between Hb9 INs in spinal cords of newborn and juvenile mice. The coupling strength varied from 2 to 32% with an average of 12%. Our data suggested that the variability was not correlated with the distribution of electrical synapses at different electronic distances. Electrical synapses behaved as low-pass filters, reducing currents passing at frequencies >3 Hz. Episodes of spontaneous bursts of EPSCs were synchronous in coupled Hb9 INs, indicating that common synaptic inputs coordinated their activity. However, non-NMDA receptor-mediated synaptic transmission was not required to synchronize neurochemically induced membrane oscillations between electrically coupled interneurons. The finding that electrical transmission persists in mice that can walk is indicative of its importance in coordinating the activity of this neuronal population in functionally mature spinal networks.

Key words: **electrical coupling; gap junction-mediated transmission; rhythm coordination; locomotor-related interneurons; excitatory spinal interneurons; mouse spinal cord**

Introduction

Electrical transmission is rare in the mature mammalian nervous system but is evident among neurons in which synchronous activity is important for function, such as between hippocampal pyramidal neurons (MacVicar and Dudek, 1981) inferior olivary neurons (Llinás and Yarom, 1986), cerebellar inhibitory neurons (Mann-Metzer and Yarom, 1999), and GABAergic neurons in the neocortex (Galarreta and Hestrin, 1999; Gibson et al., 1999). Motor behavior requires temporally coordinated activity between motoneurons innervating homonymous muscles. It has long been recognized that before the establishment of strong synaptic inputs in newborn rodents, motoneuron activity is synchronized by gap junction-mediated electrical coupling in the spinal cord (Fulton et al., 1980; Chang et al., 1999) and brainstem (Rekling and Feldman, 1997). In spinal motoneurons, as in numerous other preparations, gap junction connectivity gradually decreases as neuronal activity increases (Walton and Navarrete, 1991), and inappropriate synapses onto motoneurons are eliminated (Seebach and Ziskind-Conhaim, 1994).

Electrical synapses between interneurons are crucial for generating rhythmic motor outputs in invertebrates (Norekian, 1999; for review, see Marder, 1998), but little is known about electrical transmission between rhythmic interneurons in networks mediating motor activity in tetrapods (for review, see Kiehn and Tresch, 2002). The limited information can be at least partially attributed to difficulties identifying homogeneous populations of locomotor-related spinal interneurons. Using paired recordings, it has been shown that functionally identified rhythmogenic respiratory interneurons are electrically coupled in the pre-Bötzinger complex of newborn mice (Rekling et al., 2000).

Recently, we have characterized a genetically distinct cluster of lamina VIII interneurons expressing the Hb9 protein [Hb9 interneurons (Hb9 INs)]. Neurochemically induced locomotor-like rhythms in green fluorescent protein-positive (GFP^+) Hb9 INs are in-phase with rhythmic motor outputs (Hinckley et al., 2005b), raising the intriguing possibility that they are integral components of the locomotor central pattern generator. Based on morphological and immunohistochemical observations, we have proposed that Hb9 INs are premotor, excitatory interneurons.

Neurobiotin-filled processes of Hb9 INs are in close apposition to somata and proximal dendrites of adjacent Hb9 INs (Hinckley et al., 2005b), suggesting that the clustered interneurons are synaptically interconnected. To test this hypothesis,

Received Aug. 10, 2005; revised June 22, 2006; accepted June 24, 2006.

This work was supported by National Institutes of Health Grant NS23808 to L.Z.-C. We dedicate our paper to the memory of Prof. Robert Werman (1929–2005), a renowned scholar who made fundamental contributions to our understanding of synaptic transmission in the spinal cord. We thank Linying Wu for expert technical assistance with rhodamine staining.

Correspondence should be addressed to Dr. Lea Ziskind-Conhaim, Department of Physiology, 129 SMI, University of Wisconsin Medical School, Madison, WI 53706. E-mail: lconhaim@physiology.wisc.edu.

DOI:10.1523/JNEUROSCI.0395-06.2006

 0270-6474/06/268477-07$15.00/0

whole-cell paired recordings were performed in Hb9 INs in spinal cords of newborn stationary mice [1–4 d after birth (P1–P4)] and juvenile mice that can walk (P10–P11). Bidirectional electrical coupling was evident between the majority of Hb9 INs, and it persisted in juvenile mice with functionally mature motor activity. Moreover, our findings suggested that electrical transmission contributed to rhythm coordination between coupled Hb9 INs, independently of fast glutamatergic transmission.

A preliminary report of this study was published in an abstract form (Ziskind-Conhaim and Hinckley, 2005).

Materials and Methods

Whole-cell and population recordings. Experiments were performed using the HB9/eGFP transgenic mouse line (Wichterle et al., 2002). Newborn mice (P1–P4) were anesthetized by hypothermia, and juvenile mice (P10–P11) were anesthetized by exposure to halothane or ether. Mice were then decapitated, and spinal cords were extracted in ice-cold oxygenated extracellular solution. The procedures for whole-cell recordings from visually identified Hb9 INs in the hemisected spinal cord were identical to those described previously (Ziskind-Conhaim et al., 2003; Hinckley et al., 2005b). Simultaneous whole-cell recordings from Hb9 INs (Multiclamp 700B amplifier; Molecular Devices, Union City, CA) were performed using electrodes pulled to tip resistances of 5–7 MΩ using a multi-stage puller (P-97; Sutter Instruments, Novato, CA). Intracellular potentials/currents were filtered at 3 kHz and digitized at 10–20 kHz. Only interneurons with resting membrane potentials more negative than −50 mV and overshooting action potentials were included in this study. Membrane potentials were corrected for a 10 mV liquid junction potential (Gao et al., 2001). Population recordings from lumbar motoneurons (L1–L3 ventral roots) were identical to those described previously (Hinckley et al., 2005a).

Retrograde labeling of neurons. To retrogradely label motoneuron somata, the ventral root was placed in a tight-fitting glass pipette filled with crystals of rhodamine dextran-amine dissolved in extracellular solution (Glover et al., 1986). Incubation was for 5–8 h at room temperature. Spinal cords were then fixed in 4% paraformaldehyde in PBS overnight, and neuron labeling was examined in 100-μm-thick transverse sections.

Immunohistochemistry. Neurons expressing choline acetyltransferase (ChAT) were identified by staining with anti-ChAT antibody. Fixed sections (100 μm; see above) were incubated in 3% hydrogen peroxide and 10% methanol for 30 min and in 0.2% Triton for 10 min, followed by a 1 h incubation in 10% horse serum. All dilutions were in 0.1 M PBS. This was followed by incubation in goat anti-ChAT antibody (1:200; Chemicon, Temecula, CA), 0.1% Triton, and 0.5% horse serum for 1 h at room temperature and overnight at 4°C. Sections were then washed, blocked in 10% horse serum for 10 min, and incubated in horse biotinylated anti-goat antibody (1:200; Vector Laboratories, Burlingame, CA), 0.05% Triton, and 0.5% horse serum for 1 h. To visualize the staining, sections were incubated in ABC reagent (Vector Laboratories) and developed with DAB (Ziskind-Conhaim, 1990).

Data analysis. The coupling coefficient was measured from the ratio between the amplitude of steady-state hyperpolarizations in the postjunctional and prejunctional neurons (V_2:V) in response to a 30 pA/1 s negative current pulse in the prejunctional neuron (I_1). The junctional conductance was estimated from the current generated in the postjunctional neuron in response to a voltage command of −50 mV in the prejunctional neuron. The calculations were based on the method described by Neyton and Trautmann (1985). Junctional delays were measured between the peak action potential in the prejunctional neuron and the peak transient inward current in the postjunctional neuron. The time constant of the junctional current was measured from the onset of the current, which was best fit with a single-exponential function (Origin 6.0).

Cross-correlograms were used to evaluate the correlation between spontaneous action potentials in paired Hb9 INs. Data were resampled at 1–2.5 kHz (Hinckley et al., 2005a), and cross-correlograms were computed using Clampfit 9.2 (Molecular Devices). Histograms of instantaneous spike frequency tested the correlation between firing in Hb9 INs and the phase of the cycle period.

Solutions and chemicals. The extracellular solution contained the following (in mM): 128 NaCl, 4 KCl, 1.5 $CaCl_2$, 1 $MgSO_4$, 0.5 NaH_2PO_4, 21 $NaHCO_3$, and 30 glucose. The solution was adjusted to pH 7.3 using NaOH, and the osmolarity was 315–325 mOsm. In extracellular solution containing tetraethylammonium (TEA; 10 mM), the NaCl concentration was reduced to 118 mM and $CaCl_2$ was increased to 3 mM. The whole-cell pipette solution contained the following (in mM): 140 K-gluconate, 9 KCl, 10 HEPES, 0.2 EGTA, 1 Mg-ATP, and 0.1 GTP. The solution was adjusted to pH 7.2 using KOH, and the osmolarity was 290–305 mOsm. Neurobiotin (0.5%) was included in the pipette solution. All chemicals were obtained from Sigma (St. Louis, MO).

Results

Identification of Hb9 INs

The homeodomain transcription factor *HB9* is primarily expressed in motoneurons (Arber et al., 1999; Thaler et al. 1999). Our findings that the Hb9 protein is distinctly expressed in a group of lamina VIII interneurons in segments L1–L3 (Hinckley et al., 2005b) raised the interesting possibility that these are, in fact, a subpopulation of motoneurons. To determine whether axons of Hb9 INs projected to the periphery, motor axons were retrogradely filled with rhodamine-conjugated dextran-amine. Somatic and sympathetic motoneurons, but not Hb9 Ins, were labeled with rhodamine (Fig. 1*A*), indicating that Hb9 INs did not innervate peripheral targets. One of the criteria for motoneuron identification is the generation of antidromic action potentials in response to ventral root stimulation. The failure of ventral root stimulation to evoke action potentials in Hb9 INs ($n = 8$; data not shown) provided additional evidence that Hb9 INs do not constitute a subpopulation of motoneurons.

ChAT, the enzyme for acetylcholine biosynthesis, is frequently used as a marker for motoneuron identification. Somatic and sympathetic motoneurons were prominently stained with anti-ChAT antibody, but the staining was absent in Hb9 INs (Fig. 1*A*). These findings ruled out the possibility that Hb9 INs are cholinergic neurons. Similar data have been reported recently in juvenile Hb9/GFP mice (Wilson et al., 2005).

The morphological properties of the spindle-shaped Hb9 INs and their clustering in medial lamina VIII facilitated their visual targeting for whole-cell recordings. Common electrophysiological properties served as additional measures for their identification. These properties included the following: (1) relatively high input resistance, ranging from 700 MΩ to 1.3 GΩ (Fig. 1*B*); (2) linear current–voltage relationships at potentials more negative than −50 mV. Hyperpolarization-dependent depolarization sags were frequently recorded in adjacent interneurons but not in Hb9 INs (Fig. 1*B*); (3) small afterhyperpolarizing potentials (<10 mV); and (4) a maximal firing rate of ~25 Hz in response to prolonged positive currents and characteristic spike-frequency adaptation. For example, at 20 Hz, the interspike interval increased by an average of ~85% during the 800 ms current pulse. Based on their genetic, morphological, and electrophysiological properties, we concluded that Hb9 INs constitute a homogenous population of locomotor-related interneurons.

Bidirectional electrical coupling between Hb9 INs

To determine whether Hb9 INs were synaptically interconnected, interneurons with visible GFP^+ processes between them were targeted for paired recordings. Prolonged membrane depolarization and a train of action potentials in the injected neuron produced a relatively large DC component and spikelets correlating with each action potential in the noninjected neuron (Fig. 2).

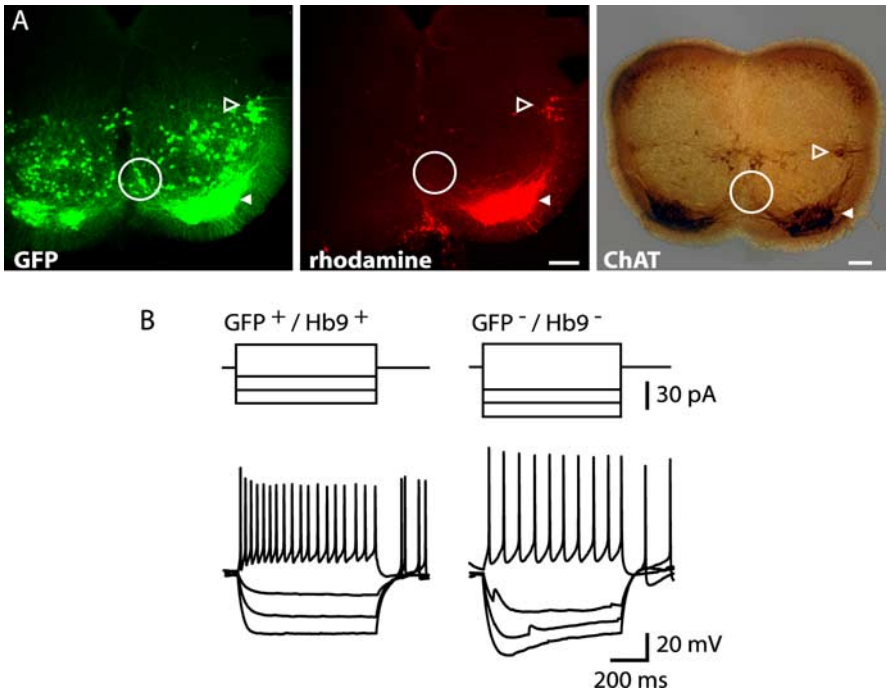

Figure 1. Characteristics of Hb9 INs. ***A***, Hb9 INs did not project to the periphery, and they did not express ChAT. Neurons with peripheral axons were retrogradely labeled with rhodamine dextran-amine. Rhodamine-filled somatic (solid arrowhead) and sympathetic (open arrowhead) motoneurons were evident, but rhodamine was absent in $GFP^+/Hb9^+$ INs (circles). In a different spinal cord, labeling with anti-ChAT antibody was apparent only in the two motoneuron populations. Scale bars, 100 μm. ***B***, Current-clamp recordings from an Hb9 IN ($GFP^+/Hb9^+$) and a neighboring $GFP^-/Hb9^-$ interneuron. Resting membrane potentials in both interneurons were approximately −60 mV. Positive current injection (30 pA/800 ms) evoked a 23 and 13 Hz repetitive firing in Hb9 and GFP^- interneurons, respectively. Spike-frequency adaptation characterized the firing in the Hb9 IN. The interspike interval between the last two spikes increased by 67% compared with the first two spikes. Typically, linear *I–V* relationships were generated in Hb9 INs at potentials more negative than the resting potential, but negative current injections produced hyperpolarization-dependent depolarization sags in the GFP^- interneuron. Input resistances were 1.2 and 1.0 GΩ for $GFP^+/Hb9^+$ and $GFP^-/Hb9^-$ interneurons, respectively.

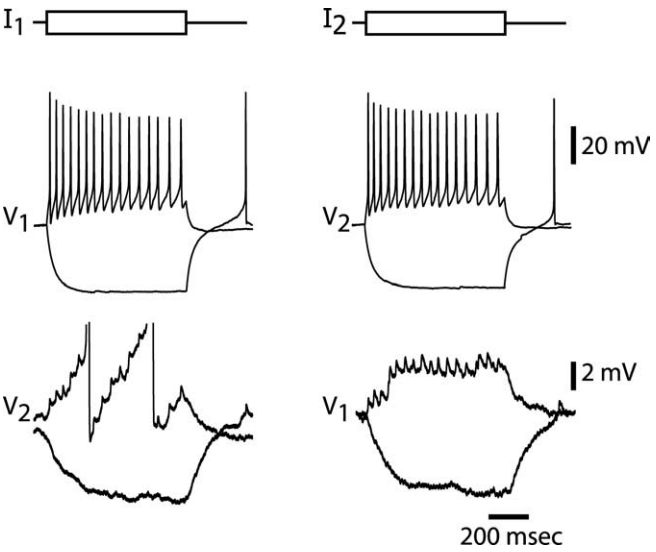

Figure 2. Bidirectional electrical coupling between Hb9 INs in the hemisected spinal cord of a P3 mouse. A long-duration positive current (30 pA/800 ms, I_1) produced a 20 Hz firing in the injected neuron (V_1) and synchronous spikelets in the postjunctional neuron (V_2). Summation of five to six spikelets reached threshold to generate two action potentials. Negative currents produced hyperpolarizations in both neurons. Similar potential changes were generated when current was injected in neuron 2 (I_2), but the spikelets in the coupled interneuron (V_1) did not reach action potential threshold. The coupling coefficient was 14.8%.

Similarly, hyperpolarization of one neuron hyperpolarized the second neuron. The transfer of positive and negative currents between the paired neurons suggested that the neurons were electrically coupled. Electrical transmission was evident between 84% of Hb9 INs in newborn mice ($n = 31$ of 37 pairs). In all coupled interneurons ($n = 31$ pairs), current passing was bidirectional so that current injection in the second neuron also produced potential changes in both neurons (Fig. 2). Electrical coupling was not detected between Hb9 INs and adjacent GFP^- interneurons ($n = 7$).

The coexistence of electrical and chemical synapses has been demonstrated in various preparations. To examine whether Hb9 INs are coupled by excitatory glutamatergic synapses, action potentials were evoked in prejunctional neurons to generate inward currents in postjunctional neurons (Fig. 3). Currents with latencies <0.3 ms and an average amplitude of 6.5 ± 1.4 pA (SE; $n = 16$) were recorded in electrically coupled interneurons. The amplitude of the evoked currents did not significantly change at various membrane potentials (e.g., −40 to −80 mV) (Fig. 3*A*). Moreover, 6-cyano-7-nitroquinoxalene-2,3-dione (CNQX, 10 μM), a non-NMDA receptor (NMDAR) antagonist that suppressed spontaneous and dorsal root-evoked EPSCs, did not block the inward currents ($n = 8$) (Fig. 3*B*). To confirm that the short-latency currents were mediated via gap junctions, recordings were performed in the presence of carbenoxolone, a gap junction blocker (Draguhn et al., 1998). Carbenoxolone did not alter the resting membrane potential or action potential properties. Exposure to carbenoxolone (100 μM) reversibly suppressed the postjunctional currents (Fig. 3*C*), with an average current reduction of 79.2 ± 0.07% (SE; $n = 7$).

The fraction of electrically coupled spinal motoneurons and the strength of transmission between them significantly decrease during the second week after birth, when juvenile rodents exhibit functionally mature motor behavior (Walton and Navarrete, 1991). To determine whether a similar developmental trend affected gap junction coupling between Hb9 INs, paired recordings were performed at P10–P11. Whole-cell recordings were difficult to obtain in older mice. In contrast to the transient coupling between spinal motoneurons, electrical transmission persisted in 83% of Hb9 INs ($n = 5$ of 6 pairs) in juvenile mice (Fig. 4*A*).

Functional properties of electrical coupling

The average distance between somata of coupled Hb9 INs was 33 μm (±3.8 SE; $n = 25$). The estimate was based on the distance between the tips of the recording electrodes. The mean time constant of the junctional currents was 2.9 ± 0.6 ms ($n = 12$). The strength of electrical synapses as estimated by calculating the coupling coefficient varied considerably (Fig. 4*B*), ranging from 2 to 32% with an average of 12.4 ± 1.6% (SE; $n = 27$) in newborn mice. Similar ratios were estimated in both directions. It is unlikely that the variability in coupling coefficients was related to

the distance of electrical synapses from the somata, because neither the time constant nor the distance between paired interneurons was correlated with the coupling coefficient ($r = 0.36$ and 0.32, respectively). An average coupling coefficient of 13.3 ± 2.4% ($n = 5$) was estimated in juvenile mice, indicating that the strength of electrical transmission did not decrease during the first 2 weeks after birth.

The junctional conductance was estimated from currents generated in postjunctional neurons in response to voltage commands of −50 mV in prejunctional neurons (Fig. 4*A*). An average conductance of 139 ± 20.7 pS (SE; $n = 12$) was calculated for coupled Hb9 INs in both newborn and juvenile mice.

To examine whether the coupling coefficient was frequency dependent as has been demonstrated in other systems (Galarreta and Hestrin, 1999; Rekling et al., 2000, Gibson et al., 2005), coupling ratios were measured at variable sine-wave frequencies (Fig. 5). The coupling coefficient decreased as a function of increased frequency to ~50% at 2–3 Hz. The functional implication of the low-pass filtering was that waveforms of fast signals such as action potentials were heavily distorted (Fig. 5*B*).

Episodes of spontaneous bursts of EPSCs and action potentials were infrequent in Hb9 INs, but in all cases they were strongly coordinated between electrically coupled Hb9 INs (Fig. 6*A*,*B*). It is reasonable to assume that common synaptic inputs triggered the onset of spontaneous bursts. Firing at 0.5–2 Hz, which was not associated with bursts of EPSCs, was also synchronized between coupled Hb9 INs (Fig. 6*C*,*D*). In the example shown, spikelet amplitudes varied from 0.8 to 2.6 mV in one interneuron and from 0.7 to 2.4 mV in the second interneuron, with averages of 1.8 mV ($n = 38$) and 1.4 mV ($n = 44$), respectively. Similar potentials that were not associated with prejunctional action potentials had mean amplitudes of 1.5 mV ($n = 28$) and 1.0 mV ($n = 8$). It is conceivable that these were spikelets generated by firing in another electrically coupled Hb9 INs. However, we could not definitively identify these as postjunctional potentials because their waveforms were similar to those of EPSPs (Fig. 5*B*).

Exposure to NMDA (4–7 μM), 5-HT (7–10 μM), and dopamine (25–50 μM) (Hinckley et al., 2005a) produced membrane oscillations and rhythmic firing in Hb9 INs that were in-phase with ventral root bursts (Fig. 7*A*). A rhythmic, twofold increase in EPSC frequency was evident during ventral root bursts, but the low frequency of IPSCs (<0.5 Hz) did not change during the cycle period Hinckley et al., 2005b, their Fig. 7. The increased EPSC frequency preceded the burst onset, raising the possibility that excitatory synaptic inputs triggered locomotor-like membrane oscillations. To determine whether rhythm onset was dependent on non-NMDAR-mediated EPSCs, experiments were conducted in the

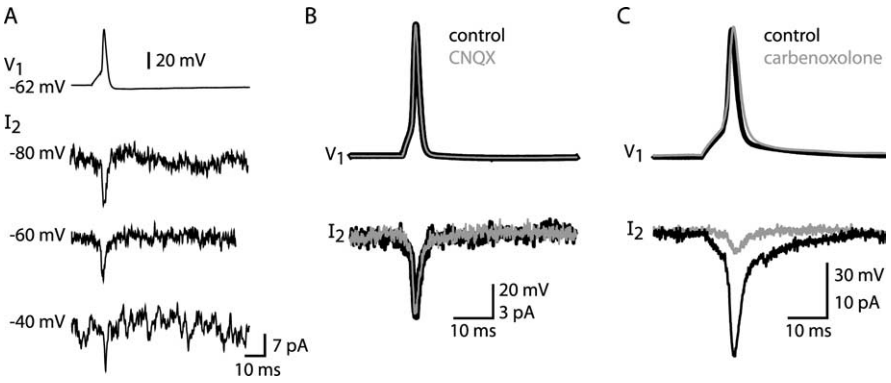

Figure 3. Electrical coupling in Hb9 INs was not associated with chemical synaptic transmission. ***A***, Action potential in the prejunctional interneuron (V_1) produced a short-latency (~0.2 ms) inward current in the postjunctional neuron (I_2) in a hemisected cord of a P3 mouse. The amplitude of the inward currents did not significantly change at holding potentials ranging from −40 to −80 mV. ***B***, Identical postjunctional inward currents were generated in the absence (black trace) and presence (gray trace) of CNQX (10 μM for 30 min) in coupled Hb9 INs in a P2 mouse. ***C***, In coupled Hb9 INs in the hemicord of a P4 mouse, the inward current was reversibly suppressed by carbenoxolone (100 μM). Recordings were performed after a 25 min exposure to the blocker. The traces in ***B*** and ***C*** are averages of 10 recordings generated at 0.1 Hz.

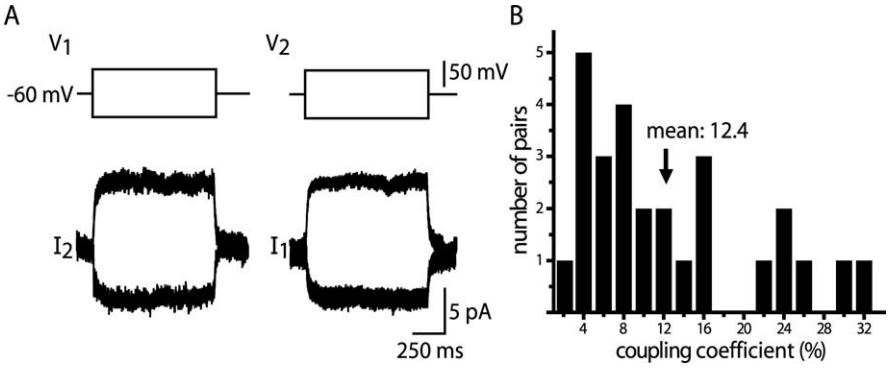

Figure 4. Electrical coupling persisted in juvenile mice. ***A***, Voltage commands of ±50 mV in a prejunctional Hb9 IN (V_1) generated currents of approximately −5/+7 pA in the postjunctional neuron (I_2) in the spinal cord of a P10 mouse. Similar currents were produced in the first Hb9 IN (I_1) in response to voltage commands in neuron 2. The smaller amplitude of the inward than outward currents might reflect differences in input resistance at depolarizing and hyperpolarizing potentials. A junctional conductance of 182 pS was measured in response to a voltage command of −50 mV. ***B***, Histogram showing a wide range of coupling coefficients between electrically coupled Hb9 INs in P1–P4 mice. The mean coupling coefficient was 12.4%.

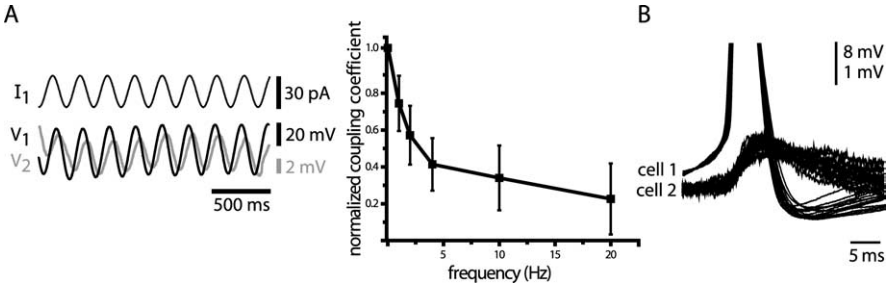

Figure 5. Electrical synapses served as low-pass filters. ***A***, Frequency-dependent transmission of sine wave current between Hb9 INs. Left, The coupling coefficient was 13.5% during a 4 Hz sine wave, corresponding to 42% of the steady-state coupling. Right, Mean coupling coefficients as a function of frequency. The coupling coefficient decreased to ~50% at 3 Hz and 30% at 20 Hz. Coupling coefficients were normalized to steady-state values. Error bars indicate SEs. ***B***, Prejunctional action potentials generated by a prolonged positive current (see Fig. 2) triggered the onset of short-latency postjunctional spikelets. Superimposed are 12 consecutive action potentials and spikelets. Action potential peaks are truncated. Spikelet amplitudes varied from 0.5 to 1.4 mV.

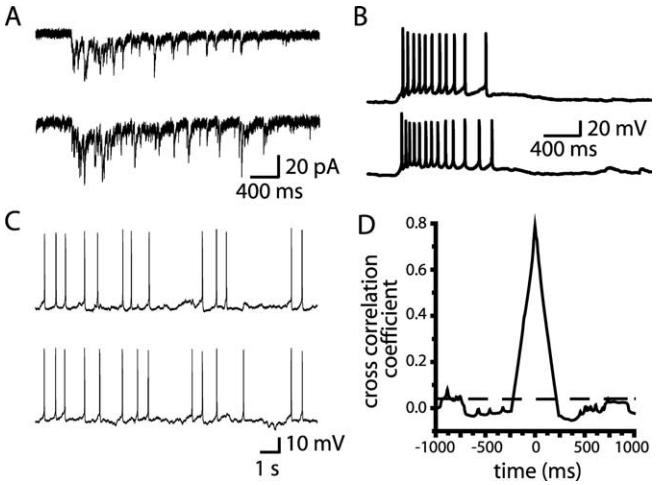

Figure 6. Episodes of synchronous EPSCs and firing in electrically coupled Hb9 INs. ***A***, Synchronized onset of burst of EPSCs in paired interneurons in a P4 mouse. The burst lasted for >2 s. The coupling coefficient was 26%. ***B***, Coordinated spontaneous firing bursts in electrically coupled Hb9 INs in a P2 mouse. The coupling coefficient was 21%. ***C***, Random firing was synchronized in the same pair of Hb9 INs shown in ***A***. ***D***, Cross-correlogram of action potential firing shown in ***C*** demonstrated a significant correlation (~0.8) of firing within ±1 ms. Although the firing correlation gradually decreased over time, it was significant over a relatively large time scale (±250 ms). The range of +3 × SE is marked by the dashed horizontal line.

presence of CNQX. CNQX-resistant membrane oscillations were recorded in 70% of Hb9 INs ($n = 7$ of 10), but ventral root bursts were suppressed. This finding suggested that neurochemically induced rhythm initiation was independent of non-NMDAR-mediated synaptic transmission.

Large, neurochemically induced membrane oscillations were generated more consistently in a low concentration of TEA (10 mM) and increased extracellular Ca^{2+} concentration (3 mM) (Fig. 7*B*). Synchronous rhythms were evident in the presence of CNQX ($n = 6$), indicating that non-NMDAR-mediated synaptic transmission was not required for rhythm coordination between electrically coupled Hb9 INs. The similar amplitude and waveform that characterized the induced rhythms in electrically coupled Hb9 INs were attributed to their homogeneous electrophysiological properties. Under these conditions, the average cycle period was 16.3 s (with a coefficient of variance of 0.2; $n = 5$), longer than the average period of 9 s reported previously (Hinckley et al., 2005b). It is conceivable that blocking TEA-sensitive K currents contributed to the longer cycle period.

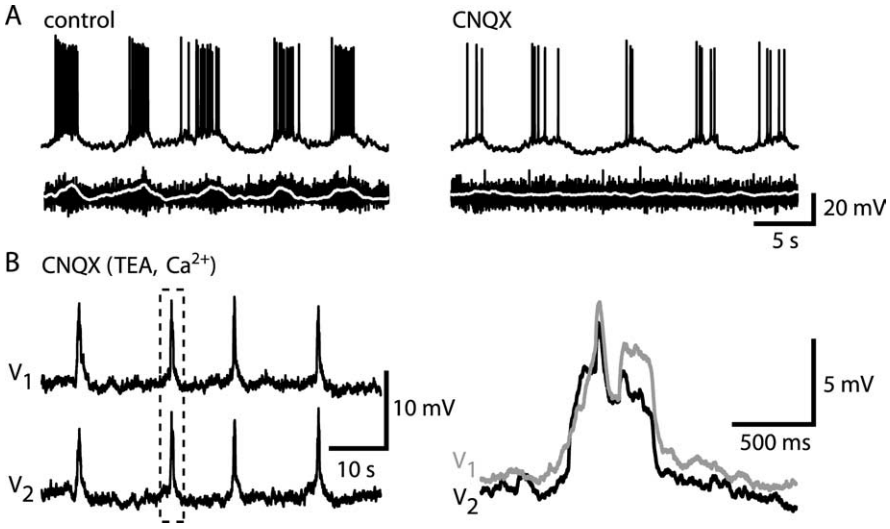

Figure 7. Neurochemically induced coordinated rhythms in electrically coupled Hb9 INs. ***A***, Membrane oscillations in-phase with ventral root bursts (bottom traces) were produced in the presence of NMA (*N*-methyl-D,L-aspartate; 5 μM), 5-HT (10 μM), and dopamine (50 μM) in a P3 mouse. The electroneurograms were rectified and smoothed using adjacent averaging over 100–200 points (white traces). Exposure to CNQX (10 μM for >30 min) did not suppress the rhythms in the Hb9 IN but eliminated motoneuron bursts. The average cycle period was 6.2 ± 0.3 s (SE; $n = 20$ cycles), not significantly different from the period recorded in the presence of CNQX (6.4 ± 0.2 s). ***B***, Neurochemically induced membrane oscillations were generated in the presence of TEA (10 mM) and higher Ca^{2+} concentration (3 mM) in a P4 mouse. The average cycle period was 19.8 ± 0.9 s ($n = 20$ cycles), and the coefficient of variance was 0.2. Rhythms with similar amplitudes and waveforms were produced, and their onset was synchronized between the coupled interneurons. Marked rhythms (dashed box) were expanded to show these properties (right).

Discussion

Bidirectional electrical coupling plays an important role in synchronizing the rhythms generated in the population of Hb9-expressing interneurons in the mouse spinal cord. Electrical transmission has been reported previously between somatic (Walton and Navarrete, 1991; Chang et al., 1999) and sympathetic (Logan et al., 1996) motoneurons in the rat spinal cord. However, to the best of our knowledge, this is the first report that demonstrates a high-incidence electrical transmission between excitatory, locomotor-related interneurons in the mammalian spinal cord. Bidirectional electrical coupling provides an effective mechanism of coordinating the activity of clustered Hb9 INs independently of non-NMDAR-mediated synaptic transmission.

Properties of electrical coupling between Hb9 INs

The properties of electrical transmission between rhythmic Hb9 INs will be discussed with reference to known characteristics of electrical synapses between other spinal neurons and neurons that comprised integral components of networks mediating rhythmic motor behavior. Electrical coupling was evident between the majority of Hb9 INs in the spinal cords of newborn (84%) and juvenile (83%) mice. The incidence of coupled Hb9 INs was significantly higher than the percentage of coupled neurons reported in other neuronal populations. Ten percent of sympathetic, preganglionic neurons were electrically coupled in the juvenile rat spinal cord (Nolan et al., 1999). A low percentage of coupling (25%) was also documented between pairs of inspiratory XII motoneurons (Rekling and Feldman, 1997) and among rhythmic type-1 inspiratory interneurons (13%) in the newborn rat (Rekling et al., 2000). The ability to visually target the GFP^+ Hb9 INs for paired recordings and confirming their identity based on electrophysiological properties decreased the probability of recording from adjacent, non-Hb9 INs.

The location of gap junctions has functional implications in signal transmission. Somatic or proximal dendritic contacts are more effective than distal contacts in current transmission because they tend to reduce signal filtering and the time for its propagation between cells. Clustered, paired Hb9 INs were closer to each other than distances reported for electrically coupled inspiratory-modulated motoneurons (50 μm) and rhythmogenic type-1 interneurons (60 μm). The rela-

tively short time constant of currents transmitted between Hb9 INs might be indicative of electrical synapses close to the somata, but other factors, not examined in this study, cannot be ruled out.

The strength of electrical coupling between Hb9 INs varied considerably, but we concluded that the variability was not related to differences in electrotonic distances. The average coupling coefficient of 12–13% was similar to that reported in various preparations including preganglionic neurons (Nolan et al., 1999), spinal interneurons in embryonic zebrafish (Saint-Amant and Drapeau, 2001), inspiratory motoneurons (Rekling and Feldman, 1997), and rhythmogenic inspiratory interneurons in newborn rats (Rekling et al., 2000). The average junctional conductance was ~140 pS. Assuming that the channels are formed by the neuronal gap junction protein connexin 36, and that the unitary channel conductance is 14 pS (Teubner et al., 2000), then only ~10 channels are generally open. It is conceivable that because of the high input resistance of Hb9 Ins, only a small number of channels need to be open to allow for an effective current transfer between the coupled neurons.

Similar to previous reports, we found that electrical synapses behaved as low-pass filters, greatly attenuating signals traveling between coupled interneurons at frequencies higher than 2–3 Hz. Because low-pass filtering allows the passing of slow potential changes, it is likely that gap junction coupling between Hb9 INs contributes to the synchronization of slow membrane oscillations such as those underlying locomotor-like rhythms (Fig. 7). A similar mechanism has been proposed for the coordination of membrane oscillations in inspiratory neurons at frequencies corresponding to the inspiratory synaptic drive (~5 Hz) (Rekling et al., 2000).

Functional significance of electrical transmission between Hb9 INs

It is generally believed that electrical synapses enhance the synchronization of subthreshold potentials and spiking among clusters of neurons (for review, see Bennett, 1997; Galarreta and Hestrin, 2001; Connors and Long, 2004). Providing direct experimental evidence that electrical transmission coordinates network activity is complicated because its role in rhythm coordination has to be isolated from the contribution of chemical synaptic inputs. Our findings that membrane oscillations persisted in the presence of CNQX implied that electrical coupling played an important role in synchronizing the activity of this homogenous population of excitatory interneurons. Gap junction-mediated electrical transmission coordinates bilateral spontaneous bursts in embryonic chick spinal cord (Milner and Landmesser, 1999), and motoneuron coordination that is independent of firing in premotor interneurons has been reported in the newborn rat spinal cord (Tresch and Kiehn, 2000).

Determining the number of electrically interconnected interneurons provides a qualitative estimate of the extent of output synchronization within the population of Hb9 INs. Numerous reports have calculated the size of coupled networks based on dye coupling (e.g., neurobiotin injection) (Devor and Yarom, 2002; Lin et al., 2003; Hornstein et al., 2004). In our studies, indirect labeling of neurons by neurobiotin diffusion during whole-cell recordings from Hb9 INs was apparent in <7% of the preparations. Therefore, dye diffusion through gap junctions cannot be used as a reliable technique to label electrically coupled Hb9 INs. It is possible to assess the number of coupled interneurons based on distinct waveforms and multiple peak amplitude histograms of postjunctional potentials (Devor and Yarom, 2002). This analytical approach could not be implemented in our study because the waveforms of postjunctional potentials in Hb9 INs were similar to those of EPSPs (Fig. 5*B*).

Electrical transmission is widespread throughout the developing mammalian nervous system (for review, see Dermietzel and Spray, 1993; Kandler and Katz, 1995), with possible roles not only in synchronizing the activity of a functional neural population but also in providing channels for intercellular diffusion of molecules such as second messengers. In the developing mammalian spinal cord and brainstem, electrical coupling between motoneurons has been proposed as the primary mechanism for coordination of motoneuron firing during movement (for review, see Kiehn and Tresch, 2002) and breathing (Rekling and Feldman, 1997; Rekling et al., 2000). However, the coupling is transient and is reduced from 77% occurrence in spinal motoneurons of newborn rats (P0–P3) to only 31% at P8–P13 (Walton and Navarrete, 1991). Moreover, its strength is significantly weaker in juvenile rats. Although electrical transmission disappears in mature spinal motoneurons, connexin expression persists into adulthood (Chang et al., 1999). The developmental trend to eliminate functional gap junctions between neonatal spinal motoneurons can be delayed by transient, botulinum-induced paralysis (Pastor et al., 2003). Furthermore, nerve injury restores the coupling among axotomized adult rat motoneurons (Chang and Balice-Gordon, 2000), suggesting that dysfunctional synaptic connections with their target muscles re-establish electrical transmission between mature motoneurons.

Based on studies of synaptic communication between motoneurons, the general consensus is that electrical coupling is widespread in the immature mammalian spinal cord, but it has a smaller role in rhythm coordination in the adult spinal cord. Our findings that bidirectional electrical transmission persists between locomotor-related excitatory interneurons in mice with functionally mature motor behavior, raises the intriguing possibility that gap junction coupling provides a mechanism of synchronizing their activity in the adult spinal cord. It will be of great interest to examine whether electrical coupling is prevalent among other spinal interneurons and serves as a fundamental mechanism of rhythm coordination in neuronal populations in the mammalian spinal cord.

References

Arber S, Han B, Mendelsohn M, Smith M, Jessell TM, Sockanathan S (1999) Requirement for the homeobox gene Hb9 in the consolidation of motor neuron identity. Neuron 23:659–674.

Bennett MVL (1997) Electrical transmission: a functional analysis and comparison with chemical transmission. In: Cellular biology of neurons, handbook of physiology, the nervous system, Vol 1 (Kandel ER, ed), pp 357–416. Baltimore: Williams and Wilkins.

Chang Q, Balice-Gordon RJ (2000) Gap junctional communication among developing and injured motor neurons. Brain Res Brain Res Rev 32:242–249.

Chang Q, Gonzalez M, Pinter MJ, Balice-Gordon RJ (1999) Gap junctional coupling and patterns of connexin expression among neonatal rat lumbar spinal motor neurons. J Neurosci 19:10813–10828.

Connors BW, Long MA (2004) Electrical synapses in the mammalian brain. Annu Rev Neurosci 27:393–418.

Dermietzel R, Spray DC (1993) Gap junctions in the brain: where, what type, how many and why? Trends Neurosci 16:186–192.

Devor A, Yarom Y (2002) Electrotonic coupling in the inferior olivary nucleus revealed by simultaneous double patch recordings. J Neurophysiol 87:3048–3058.

Draguhn A, Traub RD, Achmitz D, Jefferys JG (1998) Electrical coupling underlies high-frequency oscillations in the hippocampus in vitro. Nature 394:189–192.

Fulton BP, Miledi R, Takahashi T (1980) Electrical synapses between motoneurons in the spinal cord of the newborn rat. Proc R Soc Lond B Biol Sci 208:115–120.

Galarreta M, Hestrin S (1999) A network of fast-spiking cells in the neocortex connected by electrical synapses. Nature 402:72–75.
Galarreta M, Hestrin S (2001) Electrical synapses between GABA-releasing interneurons. Nat Rev Neurosci 2:425–433.
Gao BX, Stricker C, Ziskind-Conhaim L (2001) Transition from GABAergic to glycinergic synaptic transmission in newly formed spinal networks. J Neurophysiol 86:492–502.
Gibson JR, Beierlein M, Connors BW (1999) Two networks of electrically coupled inhibitory neurons in neocortex. Nature 402:75–79.
Gibson JR, Beierlein M, Connors BW (2005) Functional properties of electrical synapses between inhibitory interneurons of neocortical layer 4. J Neurophysiol 93:467–480.
Glover JC, Petursdottir G, Jansen JK (1986) Fluorescent dextran-amines used as axonal tracers in the nervous system of the chicken embryo. J Neurosci Methods 18:243–254.
Hinckley C, Seebach B, Ziskind-Conhaim L (2005a) Distinct roles of glycinergic and GABAergic inhibition in coordinating locomotor-like rhythms in the neonatal mouse spinal cord. Neuroscience 131:745–758.
Hinckley CA, Hartley R, Wu L, Todd A, Ziskind-Conhaim L (2005b) Locomotor-like rhythms in a genetically distinct cluster of interneurons in the mammalian spinal cord. J Neurophysiol 93:1439–1449.
Hornstein EP, Verweij J, Schnapf JL (2004) Electrical coupling between red and green cones in primate retina. Nat Neurosci 7:745–750.
Kandler K, Katz LC (1995) Neuronal coupling and uncoupling in the developing nervous system. Curr Opin Neurobiol 5:98–105.
Kiehn O, Tresch MC (2002) Gap junctions and motor behavior. Trends Neurosci 25:108–115.
Lin JY, van Wyk M, Bowala TK, Teo M-Y, Lipski J (2003) Dendritic projections and dye-coupling in dopaminergic neurons of the substantia nigra examined in horizontal brain slices from young rats. J Neurophysiol 90:2531–2535.
Llinas R, Yarom Y (1986) Oscillatory properties of guinea-pig inferior olivary neurones and their pharmacological modulation: an in vitro study. J Physiol (Lond) 376:163–182.
Logan SD, Pickering AE, Gibson IC, Nolan MF, Spanswick D (1996) Electrotonic coupling between rat sympathetic preganglionic neurones in vitro. J Physiol (Lond) 495:491–502.
MacVicar BA, Dudek FE (1981) Electrotonic coupling between pyramidal cells: a direct demonstration in rat hippocampal slices. Science 213:782–785.
Mann-Metzer P, Yarom Y (1999) Electronic coupling interacts with intrinsic properties to generate synchronized activity in cerebellar networks of inhibitory interneurons. J Neurosci 19:3298–3306.
Marder E (1998) Electrical synapses: beyond speed and synchrony to computation. Curr Biol 8:R795–R797.
Milner LD, Landmesser LT (1999) Cholinergic and GABAergic inputs drive patterned spontaneous motoneuron activity before target contact. J Neurosci 19:3007–3022.
Neyton J, Trautmann A (1985) Single-channel currents of an intercellular junction. Nature 317:331–335.
Nolan MF, Logan SD, Spanswick D (1999) Electrophysiological properties of electrical synapses between rat sympathetic preganglionic neurones in vitro. J Physiol (Lond) 519:753–764.
Norekian TP (1999) GABAergic excitatory synapses and electrical coupling sustain prolonged discharges in the prey capture neural network of *Clione limacina*. J Neurosci 19:1863–1875.
Pastor AM, Mentis GZ, De La Cruz RR, Diaz E, Navarrete R (2003) Increased electrotonic coupling in spinal motoneurons after transient botulinum neurotoxin paralysis in the neonatal rat. J Neurophysiol 89:793–805.
Rekling JC, Feldman JL (1997) Bidirectional electrical coupling between inspiratory motoneurons in the newborn mouse nucleus ambiguus. J Neurophysiol 78:3508–3510.
Rekling JC, Shao XM, Feldman JL (2000) Electrical coupling and excitatory synaptic transmission between rhythmogenic respiratory neurons in the preBotzinger complex. J Neurosci 20:RC113(1–5).
Saint-Amant L, Drapeau P (2001) Synchronization of an embryonic network of identified spinal interneurons solely by electrical coupling. Neuron 31:1035–1046.
Seebach BS, Ziskind-Conhaim L (1994) Formation of transient inappropriate sensorimotor synapses in developing rat spinal cords. J Neurosci 14:4520–4528.
Teubner B, Degen J, Söhl G, Güldenagel M, Bukauskas FF, Trexler EB, Verselis VK, De Zeeuw CI, Lee CG, Kozak CA, Petrasch-Parwez E, Dermietzel R, Willecke K (2000) Functional expression of the murine connexin 36 gene coding for a neuron-specific gap junctional protein. J Membr Biol 176:249–262.
Thaler J, Harrison K, Sharma K, Lettieri K, Kehrl J, Pfaff SL (1999) Active suppression of interneuron programs within developing motor neurons revealed by analysis of homeodomain factor HB9. Neuron 23:675–687.
Tresch MC, Kiehn O (2000) Motor coordination without action potentials in the mammalian spinal cord. Nat Neurosci 3:593–599.
Walton KD, Navarrete R (1991) Postnatal changes in motoneurone electrotonic coupling studied in the in vitro rat lumbar spinal cord. J Physiol (Lond) 433:283–305.
Wichterle H, Lieberam I, Porter JA, Jessell TM (2002) Directed differentiation of embryonic stem cells into motor neurons. Cell 110:385–397.
Wilson JM, Hartley R, Maxwell DJ, Todd AJ, Lieberam I, Kaltschmidt JA, Yoshida Y, Jessell TM, Brownstone RM (2005) Conditional rhythmicity of ventral spinal interneurons defined by expression of the Hb9 homeodomain protein. J Neurosci 25:5710–5719.
Ziskind-Conhaim L (1990) NMDA receptors mediate poly- and monosynaptic potentials in motoneurons of rat embryos. J Neurosci 10:125–135.
Ziskind-Conhaim L, Hinckley CA (2005) Electrical coupling between rhythmic HB9-expressing interneurons in the mammalian spinal cord. Soc Neurosci Abstr 31:516.11.
Ziskind-Conhaim L, Gao BX, Hinckley C (2003) Ethanol dual modulatory actions on spontaneous postsynaptic currents in spinal motoneurons. J Neurophysiol 89:806–813.